SESSION 6a.

GENERAL METHODS

Session Chairman

G. G. Pope

Royal Aircraft Establishment
Farnborough, England

A METHOD OF SOLUTION FOR THE COMPLICATED BUCKLING PROBLEMS OF ELASTIC PLATES WITH COMBINED USE OF RAYLEIGH-RITZ'S PROCEDURE IN THE FINITE ELEMENT METHOD

T. Kawai* and H. Ohtsubo**

Institute of Industrial Science, University of Tokyo,

Tokyo, Japan

This paper presents a practical method of solution of the complicated elastic plate buckling problems. In the present method, initial in-plane stress distribution before buckling is obtained by means of the finite element method. Using the obtained stress distribution a critical stress is determined by the well-known Rayleigh-Ritz's procedure. To reduce the labour of numerical calculations, the double integrations encountered in the energy procedure are transformed into line integrals by the help of Gauss' theorem. For the numerical examples, buckling problems of simply-supported perforated square plates with various in-plane boundary conditions are studied and the calculated results are compared with several previous investigations.

*Associate Professor
**Graduate Student

SECTION I

SUMMARY

The finite element method has been accepted as the most practical and reliable for analysis of two dimensional stress fields. However, analysis of plate bending problems by this method has not been well established due to lack of reliable stiffness matrix of a triangular element for plate bending. Henceforth this is also true in the case of plate buckling problems. In view of the present state of art, a practical method of solution is proposed for analysis of complicated problems of plate buckling by using Rayleigh-Ritz's procedure with the initial stress distribution determined by the finite element method.

In energy solution of the plate problem, considerable time and labour are usually needed for accurate evaluation of various terms of energy integrals, and it often presents serious difficulty in the practical application. With the present method such difficulties can be overcome through their transformation into the line integrals along the plate element boundaries by using the well-known Gauss' theorem.

As for examples, buckling strength of a perforated square plate with various boundary conditions under uniaxial compression are studied in comparison with the results of previous investigation carried out by various authors.

SECTION II

RAYLEIGH-RITZ'S PROCEDURE FOR ELASTIC PLATE BUCKLING PROBLEMS

The elastic plate buckling problems can be solved by using the following variational equation:

$$\frac{D}{2}\,\delta\iint_{\Omega}\left[\left(\frac{\partial^2 w}{\partial x^2}+\frac{\partial^2 w}{\partial y^2}\right)^2-2(1-\nu)\left\{\frac{\partial^2 w}{\partial x^2}\frac{\partial^2 w}{\partial y^2}-\left(\frac{\partial^2 w}{\partial x\,\partial y}\right)^2\right\}\right]dx\,dy$$

$$+\lambda\delta\iint_{\Omega}\left[N_x^{(o)}\frac{1}{2}\left(\frac{\partial w}{\partial x}\right)^2+N_y^{(o)}\frac{1}{2}\left(\frac{\partial w}{\partial y}\right)^2+N_{xy}^{(o)}\frac{\partial w}{\partial x}\frac{\partial w}{\partial y}\right]dx\,dy=0 \tag{1}$$

Where the conventional engineering notations are employed. $(N_x^{(o)}, N_y^{(o)}, N_{xy}^{(o)})$ is the internal stress distribution induced by a certain standard load applied to plate edges, the value of which multiplied by λ_{cr} gives the critical stress distribution at onset of buckling. Where λ_{cr} stands for the minimum eigenvalue of Equation 1.

Now it is assumed that the deflection w(x,y) can be expanded into the power series of x and y as follows:

$$\left.\begin{aligned} w(x,y) &= \sum_{i=1}^{N} a_i s_i(x,y) \\ s_i(x,y) &= \phi(x,y)\,x^m y^n \end{aligned}\right\} \tag{2}$$

Where $\phi(x,y)$ is a certain function introduced which satisfies the prescribed geometrical boundary condition. After substituting Equation 2 into Equation 1, variations are taken for each coefficient a_i, resulting into the following matrix equation:

$$\mathbf{P}\,\mathbf{u} = \lambda\,\mathbf{Q}\,\mathbf{u} \tag{3}$$

where

$$\mathbf{P}=\left[\,D\,\Phi_{ij}\,\right],\quad \mathbf{Q}=\left[-\Psi_{ij}\right],\quad \mathbf{u}=\left[a_i\right]$$

and

$$\Phi_{ij}=\iint_{\Omega}\left[\frac{\partial^2 S_i}{\partial x^2}\frac{\partial^2 S_j}{\partial x^2}+\nu\left(\frac{\partial^2 S_i}{\partial x^2}\frac{\partial^2 S_j}{\partial y^2}+\frac{\partial^2 S_j}{\partial x^2}\frac{\partial^2 S_i}{\partial y^2}\right)+\frac{\partial^2 S_i}{\partial y^2}\frac{\partial^2 S_j}{\partial y^2}\right.$$

$$\left.+2(1-\nu)\frac{\partial^2 S_i}{\partial x\,\partial y}\frac{\partial^2 S_j}{\partial x\,\partial y}\right]dx\,dy \tag{4}$$

$$\Psi_{ij}=\iint_{\Omega}\left[N_x^{(o)}\frac{\partial S_i}{\partial x}\frac{\partial S_j}{\partial x}+N_y^{(o)}\frac{\partial S_i}{\partial y}\frac{\partial S_j}{\partial y}+N_{xy}^{(o)}\left(\frac{\partial S_i}{\partial x}\frac{\partial S_j}{\partial y}+\frac{\partial S_j}{\partial x}\frac{\partial S_i}{\partial y}\right)\right]dx\,dy \tag{5}$$

When the initial stress distribution ($N_x^{(o)}$, $N_y^{(o)}$, $N_{xy}^{(o)}$) is obtained by the finite element analysis based on triangular plate elements of constant stresses, Φ_{ij} can be represented by total sum of the double integrals with respect to each triangular element. Evaluation of Φ_{ij} and Φ_{ij} can be greatly facilitated by the digital computer based on the transformation formula to be developed in the following section.

SECTION III

TRANSFORMATION OF DOUBLE INTEGRALS INTO LINE INTEGRALS

Consider the following double integral:

$$I_{mn} = \int\int_{\Omega} x^m y^n \, dx \, dy \tag{6}$$

Using the following Gauss' theorem in two-dimensional field:

$$\int\int_{\Omega} \frac{\partial F(x,y)}{\partial x} \, dx \, dy = \oint_c F(x,y) \cos(n,x) \, dS$$

I_{mn} can be transformed into the following line integral:

$$I_{mn} = \frac{1}{m+1} \oint_c x^{m+1} y^n \cos(n,x) \, dS \tag{7}$$

Where Ω, c and s denote the integral domain, boundary curve and line element respectively as shown in Figure 1, and (n,x) and (s,x) stand for the angles between the normal n and the tangent s to the boundary curve, and x axis respectively. Equation 7 is valid for the multiply-connected plate region if $\oint_c$ implies the total sum of the line integrals with respect to each boundary curve where the direction of s should be properly defined.

Assuming that the plate Ω is simply-connected and denoting the angle (s,x) by θ, I_{mn} can be also rewritten as follows:

$$I_{mn} = \frac{1}{m+1} \oint_c x^{m+1} y^n \tan\theta \, dx = \frac{1}{m+1} \oint_c x^{m+1} y^n \, dy \tag{8}$$

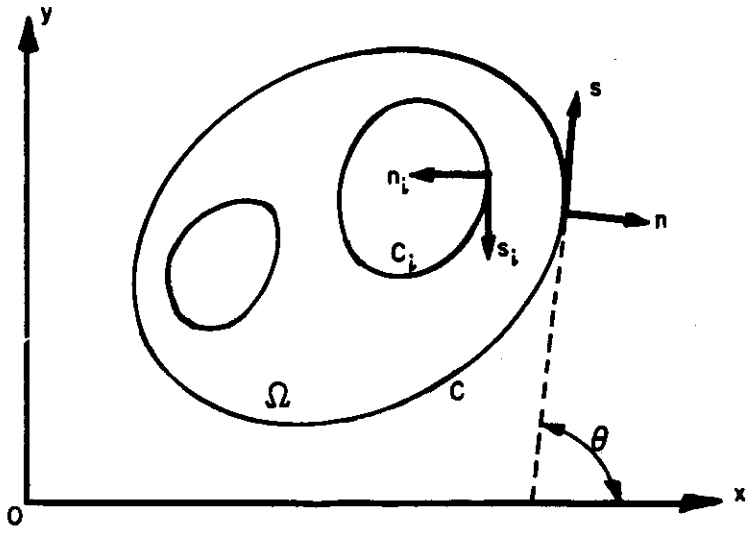

Figure 1. Integral Domain Ω, Boundary Tangent s and Normal n

Representing the boundary curve approximately by a number of straight lines $P_o P_i -- P_k$ which connect the finite number of points

$$P_o(x_o, y_o),\ P_1(x_1, y_1), \cdots, P_k(x_k, y_k) = P_o(x_o, y_o)$$

successively as shown in Figure 2. I_{mn} can be now given by the following approximate formula:

$$I_{mn} \doteq \frac{1}{m+1} \sum_{i=1}^{K} \int_{x_{i-1}(\Gamma_i)}^{x_i} x^{m+1} y^n \tan\theta_i \, dx$$

$$= \frac{1}{m+1} \sum_{i=1}^{K} \int_{y_{i-1}(\Gamma_i)}^{y_i} x^{m+1} y^n \, dy \qquad (9)$$

Where Γ_i is the ith side of the approximated polygonal boundary and is generally expressed as follows:

$$\left.\begin{aligned} y &= A_i x + B_i \\ \text{or} \quad x &= C_i y + D_i \end{aligned}\right\} \qquad (10)$$

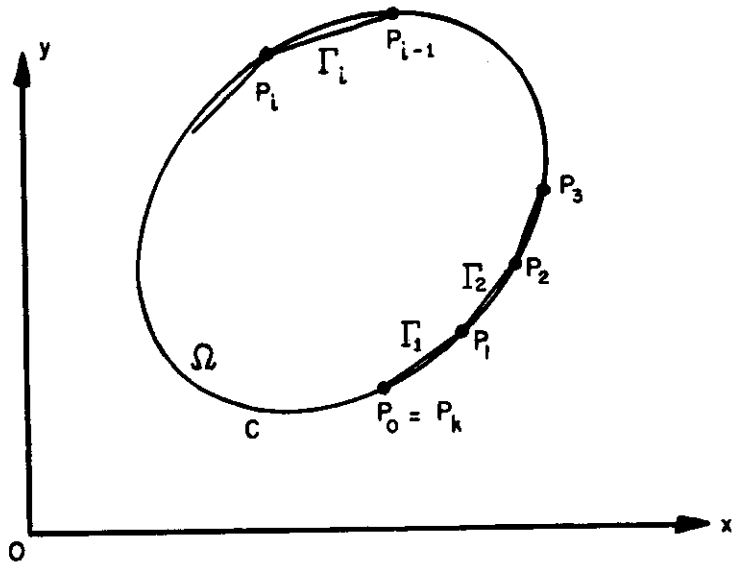

Figure 2. Approximate Representation of a Integral Domain by a Polygon

Naturally Equation 10 will be exact for the case of polygonal domain. Care must be exercised for selection of the first and the second expression given by Equation 10 in order to avoid overflow in the actual numerical calculation. For example, in case where a segment of boundary lines exists in the shaded region as shown Figure 3, the first expression will be preferable. Suppose that Γ_i is expressed by the first equation:

$$\left.\begin{aligned} A_i &= \frac{y_i - y_{i-1}}{x_i - x_{i-1}} \\ B_i &= y_{i-1} - \left(\frac{y_i - y_{i-1}}{x_i - x_{i-1}}\right) x_{i-1} \end{aligned}\right\} \tag{11}$$

and

$$\left| A_i \right| \leq 1$$

Using the binominal theorem, the line integral on the segment of boundary lines Γ_i can be calculated as follows:

1. in case where $A_i \neq 0$, $B_i \neq 0$

$$\int_{x_{i-1}(\Gamma_i)}^{x_i} x^{m+1} y^n \tan\theta_i \, dx = \int_{x_{i-1}}^{x_i} x^{m+1} (A_i x + B_i)^n A_i \, dx$$

$$= \sum_{r=0}^{n} {}_nC_r \left(\frac{y_i - y_{i-1}}{x_i - x_{i-1}}\right)^{n+1-r} \left\{y_{i-1} - \left(\frac{y_i - y_{i-1}}{x_i - x_{i-1}}\right) x_{i-1}\right\}^r \left(\frac{x_i^{m+n+2-r} - x_{i-1}^{m+n+2-r}}{m+n+2-r}\right) \tag{12}$$

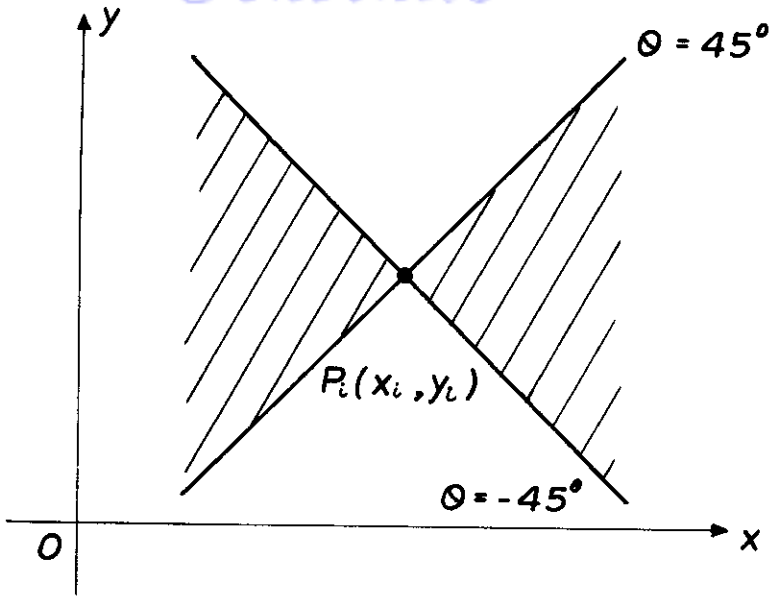

Figure 3. The Range of Application of Equation 10

2. in case where $A_i = 0$, the integral vanishes.

3. in case where $A_i \neq 0$, $B_i = 0$

$$\int_{x_{i-1}}^{x_i} x^{m+1} y^n \tan\theta_i \, dx = \frac{1}{m+n+2} \left(\frac{y_i - y_{i-1}}{x_i - x_{i-1}}\right)^{n+1} \left(x_i^{m+n+2} - x_{i-1}^{m+n+2}\right) \tag{13}$$

In the similar way, the following results can be derived when Γ_i is expressed by $x = C_i y + D_i$.

4. in case where $C_i \neq 0$, $D_i \neq 0$

$$\int_{y_{i-1}(\Gamma_i)}^{y_i} x^{m+1} y^n \, dy = \sum_{r=0}^{m+1} C_r \left(\frac{x_i - x_{i-1}}{y_i - y_{i-1}}\right) \left(x_{i-1} - \frac{x_i - x_{i-1}}{y_i - y_{i-1}} y_{i-1}\right)^r \times \frac{\left(y_i^{m+n+2-r} - y_{i-1}^{m+n+2-r}\right)}{m+n+2-r} \tag{14}$$

5. in case where $C_i = 0$

$$\int_{y_{i-1}}^{y_i} x^{m+1} y^n \, dy = \frac{1}{n+1} \left(x_i - \frac{x_i - x_{i-1}}{y_i - y_{i-1}} y_i\right)^{m+1} \left(y_i^{n+1} - y_i^{n+1}\right) \tag{15}$$

6. in case where $C_i \neq 0$, $D_i = 0$

$$\int_{y_{i-1}}^{y_i} x^{m+1} y^n \, dy = \frac{1}{m+n+2} \left(\frac{x_i - x_{i-1}}{y_i - y_{i-1}}\right)^{m+1} \left(y_i^{m+n+2} - y_{i-1}^{m+n+2}\right) \tag{16}$$

7. in case where $C_i = D_i = 0$, the integral vanishes obviously.

Equations 12 through 16 can be successfully applied to numerical integration of any polynomial of x and y defined in a given region regardless of the boundary shape. Thus a standard program for evaluation of Φ_{ij}, Ψ_{ij} in Equations 4 and 5 with respect to arbitrary plate domain can be developed.

It should be noted here that the above calculation is approximate if the boundary is represented by a single curve or a number of curves, and an estimation of the error is usually difficult, but it may be considered that the more accurate integral value can be obtained with the finer polygonal representation of the acutual boundary curve.

The critical value can be obtained directly by working the program on the following input data;

1. The coordinates of the vertices of the polygonal plate.

2. The types of geometrical boundary condition for deflection w with respect to each side segment (free, simply-supported, clamped).

3. Finite element presentation of a given plate (the coordinates and the numbering of the nodes) and the derived plane stress distribution of the idealized plate.

4. The necessary number of the approximate terms for the deflection w and the powers of x and y of the respective terms.

The basic program steps leading to the calculation in the present method are outlined in the following way:

1. Determination of the function ϕ (x,y) which satisfies the prescribed geometrical boundary condition for deflection.

2. Calculation of $\dfrac{\partial^2 S_i}{\partial x^2}, \dfrac{\partial^2 S_i}{\partial y^2}, \dfrac{\partial^2 S_i}{\partial x \partial y}$

by differentiating $S_i(x,y) = \phi(x,y)\, x^m y^n$

3. Multiplication of respective terms derived in 2.

$$\frac{\partial^2 S_i}{\partial x^2}\frac{\partial^2 S_j}{\partial x^2}, \quad \frac{\partial^2 S_i}{\partial x^2}\frac{\partial^2 S_j}{\partial y^2}, \quad \frac{\partial^2 S_j}{\partial x^2}\frac{\partial^2 S_i}{\partial y^2}, \quad \frac{\partial^2 S_i}{\partial x \partial y}\frac{\partial^2 S_j}{\partial x \partial y}$$

4. Calculation of the integrand.

$$\frac{\partial^2 S_i}{\partial x^2}\frac{\partial^2 S_j}{\partial x^2} + \nu\left(\frac{\partial^2 S_i}{\partial x^2}\frac{\partial^2 S_j}{\partial y^2} + \frac{\partial^2 S_j}{\partial x^2}\frac{\partial^2 S_i}{\partial y^2}\right) + \frac{\partial^2 S_i}{\partial y^2}\frac{\partial^2 S_j}{\partial y^2} + 2(1-\nu)\frac{\partial^2 S_i}{\partial x\,\partial y}\frac{\partial^2 S_j}{\partial x\,\partial y}$$

5. Calculation of Φ_{ij}.

The similar steps can be described for determination of Ψ_{ij}. The characteristic equation defined by Equation 3 is solved by Jacobi's method in the present procedure.

SECTION IV

SOME NUMERICAL EXAMPLES

As for example, the buckling strength of a perforated square plate under three different boundary as well as loading conditions are analyzed by using the present method. The results obtained will be compared with those of previous investigation carried out by three different authors.

THE BUCKLING OF A SQUARE PLATE SUBJECT TO UNIFORM CONSTANT STRESS

For the first numerical example, simple problems on the plate buckling of a square plate with various bending boundary conditions under uniform edge compression in two directions are considered in order to investigate the convergence of this method.

In this case the stress distribution inside of the plate is clearly given as follows:

$$N_x^{(o)} = N_y^{(o)} \quad , N_{xy}^{(o)} = 0 \tag{17}$$

The critical stresses are calculated by using this stress distribution and by taking the first six terms of the power series for the deflection function. The results obtained are shown in Table I in comparison with the results of previous investigation. The convergency of the present method is examined by taking a simply-supported square plate and it is found that three terms approximation will be sufficient for practical purpose as shown in Table II.

THE BUCKLING OF A SIMPLY-SUPPORTED PERFORATED PLATE UNDER VARIOUS LOADING CONDITIONS

The effect of the lightening holes on the plate buckling strength has been one of the most important problems in design of thin-walled structures. But so far no reliable solution procedure have been established for such problems. In this section the three types of the buckling problems of a perforated square plate with all four simply-supported edges are studied by the present method. Each one of these problems have been studied by three different authors respectively (References 2, 3, and 4). Following are the results of the present study briefly described in comparison with the previous investigation.

BOUNDARY CONDITION	σ_{cr}/σ_e	$\phi\ (x,y)$	DEFLECTION $w(x,y)$ $\left[x\,\phi(x,y)\right]$
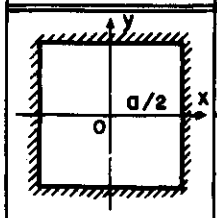	5.4024 5.304 (Faxen) 5.3036 (Iguchi)	$\left(x^2-\frac{a^2}{4}\right)^2\left(y^2-\frac{a^2}{4}\right)^2$	$1.0000-0.0004\frac{x^2}{(a/2)^2}-0.0004\frac{y^2}{(a/2)^2}$ $-0.0001\frac{x^4}{(a/2)^4}-0.0000\frac{x^2y^2}{(a/2)^4}-0.0001\frac{y^4}{(a/2)^4}$
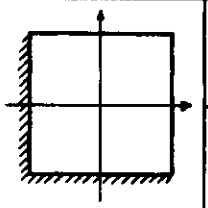	3.2603 3.2316 (Iwafuji)	$\left(x-\frac{a}{2}\right)\left(x+\frac{a}{2}\right)^2\left(y-\frac{a}{2}\right)$ $\times\left(y+\frac{a}{2}\right)^2$	$0.9775-0.1471\frac{x}{a/2}-0.1471\frac{y}{a/2}$ $-0.0170\frac{x^2}{(a/2)^2}+0.0236\frac{xy}{(a/2)^2}-0.0170\frac{y^2}{(a/2)^2}$
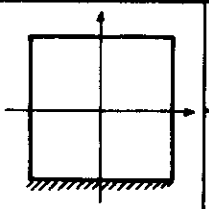	2.6631 2.69 (Iwafuji) 2.6627 (Iguchi)	$\left(x^2-\frac{a^2}{4}\right)\left(y-\frac{a}{2}\right)\left(y+\frac{a}{2}\right)^2$	$0.9854-0.1631\frac{y}{a/2}-0.0346\frac{x^2}{(a/2)^2}$ $-0.0320\frac{y^2}{(a/2)^2}+0.0060\frac{x^2y}{(a/2)^3}+0.0097\frac{y^3}{(a/2)^3}$
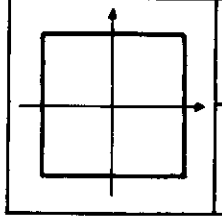	2.0000 exact solution 2	$\left(x^2-\frac{a^2}{4}\right)\left(y^2-\frac{a^2}{4}\right)$	$0.9984-0.0398\frac{x^2}{(a/2)^2}-0.0398\frac{y^2}{(a/2)^2}$ $+0.0012\frac{x^4}{(a/2)^2}+0.0014\frac{x^2y^2}{(a/2)^4}+0.0012\frac{y^4}{(a/2)^4}$

$$\sigma_e = \frac{E\pi^2}{12(1-\nu^2)}\left(\frac{h}{a}\right)^2$$

TABLE I

BUCKLING OF A SQUARE PLATE SUBJECT
TO UNIFORM CONSTANT STRESS

NO. OF TERMS	1	2	3	4	5	6
DEGREE OF TERM	1	x^2	y^2	x^4	$x^2 y^2$	y^4
MINIMUM EIGENVALUE	2.2291	2.1152	2.0008	2.0004	2.0001	2.0000
ERROR	11.45 %	5.76 %	0.04 %	0.02 %	0.01 %	0.00 %

EXACT SOLUTION 2.0

TABLE II

CONVERGENCY OF CRITICAL STRESS OF A SIMPLE-SUPPORTED SQUARE PLATE

A Perforated Plate Subject to Uniform Edge Displacement (I)

(Comparison with A. L. Schlack, Jr.'s study, Reference 2)

A. L. Schlack, Jr. carried out buckling test of a perforated square plate by using an aluminum plate 19 in. x 19 in. x 1/8 in. with Young's modulus 9.95 x 10 psi, and Poisson's ratio 0.35. All edges of the test plate are supported by a series of bearing block containing needle bearings to provide simply-supported edges and reinforcing rods are placed on each side of the plate to prevent lateral movement of the side supports. That is, the boundary condition of Schlack's experiment is considered as follows: Along AD and BC edges of the plate in Figure 4 are restrained against displacement in x-direction, while AB and CD edges are compressed under the condition of uniform displacement. All edges are simply-supported for plate deflection w.

Schlack used Rayleigh-Ritz's procedure for determination of the critical stress in which he employed three-term polynomials of x and y for in-plane displacements u, v, while four-term polynomials for plate deflection w.

It can be generally considered that his displacement functions especially in-plane ones may not be sufficient for reliable determination of the critical stress, although a fairly good agreement between his theory and test results is observed for the cases of small hole in Figure 6. For a plate with a larger hole his displacement functions seem to give too conservative critical stresses in comparison with his test results.

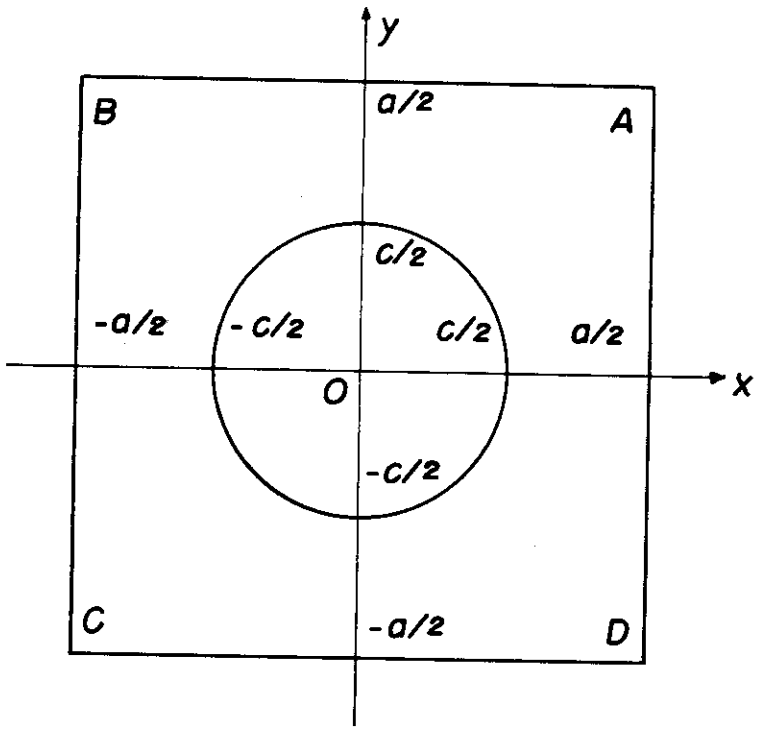

Figure 4. A Perforated Square Plate

In the present method stress distribution of a given plate under prescribed edge movement is first analyzed by using triangular discrete elements. Considering the symmetry, it can be concluded that all the necessary calculation with respect to a quarter of the total plate area will be sufficient for the present problem. Figure 5 shows a typical example of the finite element representation of a given plate. The various energy integrals involving the initial stresses can be evaluated by carrying out the line integration with respect to each triangular element inside of which constant stress condition exists and summing up all the integral values throughout the plate. The plate deflection w for symmetric buckling wave is assumed as follows:

$$w(x,y) = \left(x^2 - \frac{a^2}{4}\right)\left(y^2 - \frac{a^2}{4}\right)(a_1 + a_2 x^2 + a_3 y^2 + a_4 x^4 + a_5 x^2 y^2 + a_6 y^4 + a_7 x^6 + a_8 x^4 y^2 + a_9 x^2 y^4 + a_{10} y^6 + \cdots) \quad (18)$$

Correlation of the analytical as well as experimental results are studied as shown in Figure 6 by changing the ratio of the side length a to diameter of the circular hole c. Where $\bar{\sigma}_{cr}$ is a mean critical stress which is the quotient of the critical load by cross sectional area of the boundary edge ah and

$$\sigma_e = \frac{E\pi^2}{12(1-\nu^2)}\left(\frac{h}{a}\right)^2 \quad (19)$$

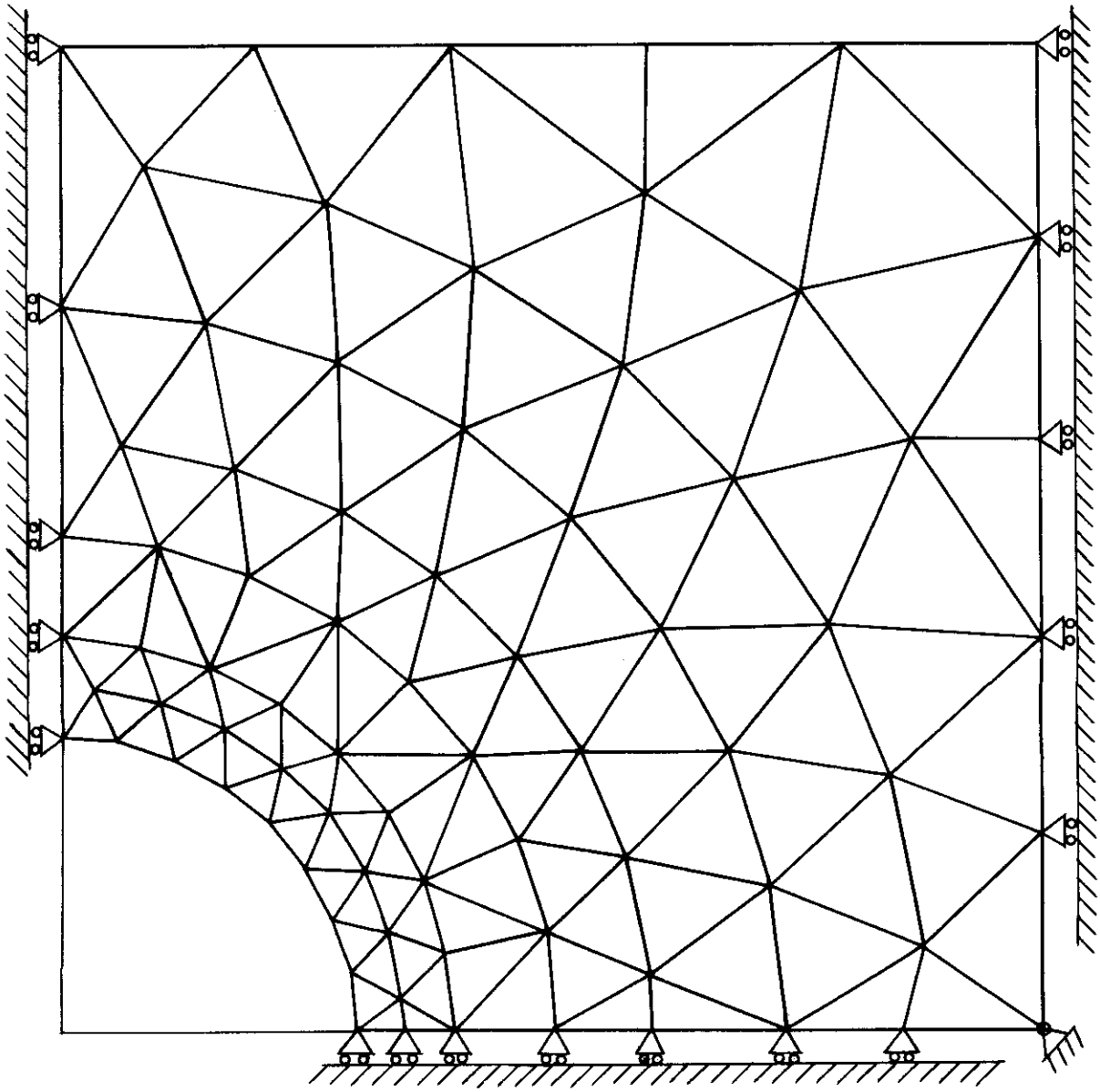

Figure 5. Idealization of a Perforated Square Plate by Triangular Finite Elements (r = 0.3)

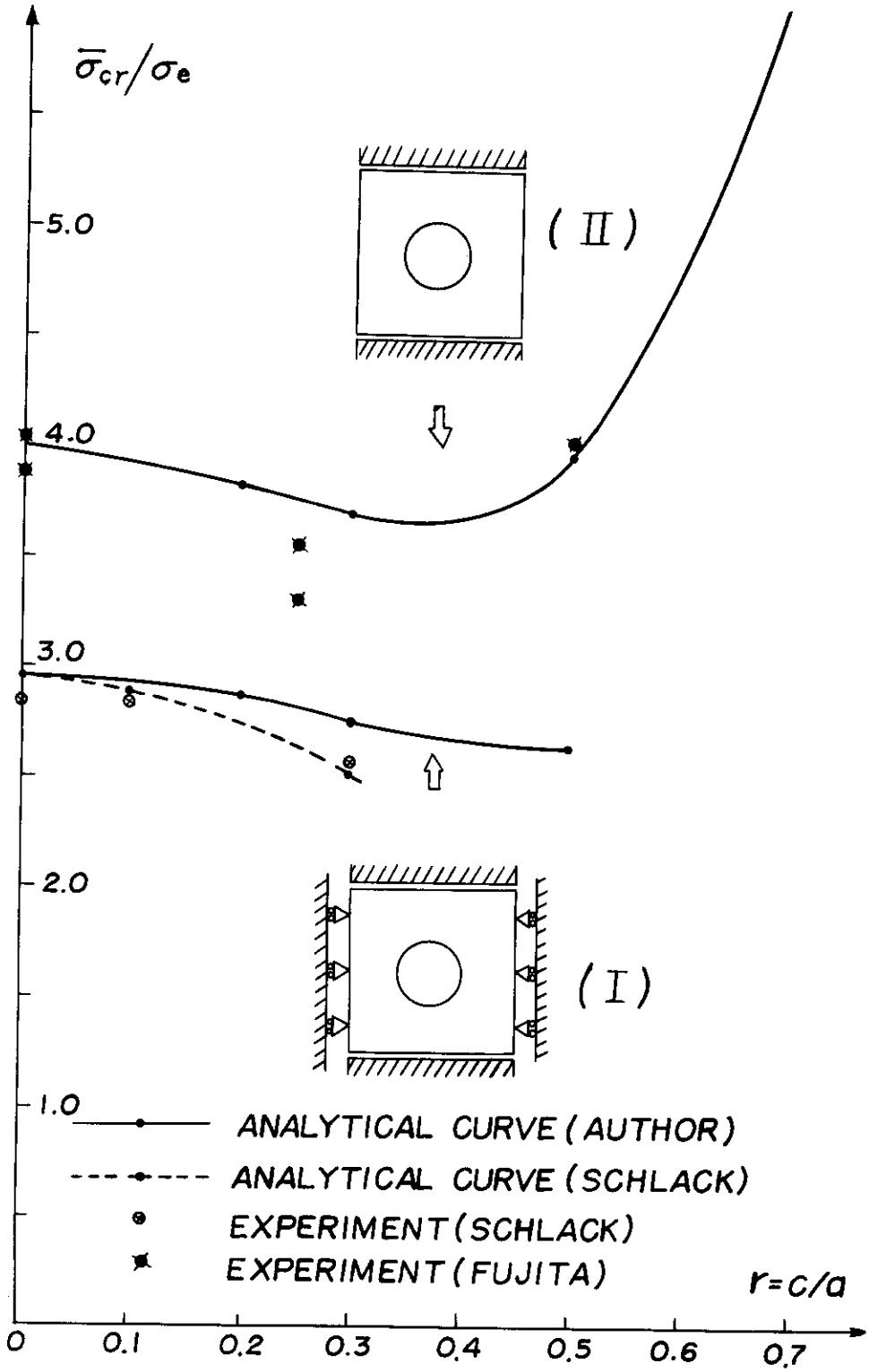

Figure 6. Critical Stress of a Simply-Supported Perforated Plate Subject to Uniform Displacement Versus Diameter of Circular Hole

In case of a square plate without a hole, the exact solution can be obtained and in this case it is 2.96296 σ_e with Poisson's ratio 0.35. For the check of overall numerical accuracy of the proposed method, the same problem is analyzed by using the 48-finite-element representation for one quadrant and a six term approximation for the plate buckling mode, this calculation results in 2.9630 σ_e.

In this study fairly good agreement with Schlack's experiments is generally observed and practical application of the present method to engineering problems can be duly justified. Figure 7 indicates the convergency of the approximate solutions to the exact solution for the case of $r = c/a = 0$ in which the minimum eigenvalues obtained are plotted against the number of terms in the plate deflection function. It can be seen from this figure that only a three-term approximation for the plate deflection will be sufficient for the practical purpose as in the previous example. In the similar way, the convergency for the case of $r = 0.3$ is shown in Figure 9. Although the corresponding exact solution has not been obtained, the similar conclusion will be drawn, judging from the monotonous convergency of the calculated results.

The Perforated Plate Subject to Uniform Edge Displacement (II)

(Comparison with Y. Fujita's study, Reference 3)

Y. Fujita et. al. made a study in 1966 on the buckling strength of a simply-supported perforated plate under uniform edge displacement with no restraint against the lateral movement of vertical plate edges as shown in Figure 4. He carried out buckling test of steel plates whose dimensions are 600 x 600 x 6.6mm and Young's modulus and Poisson's ratio are 2.17×10^4 kg/mm^2 and 0.3 respectively. The experimental load-deflection curves as well as the converted critical loads corresponding to the experiments are shown in Figures 9, and 10. The experimental critical loads were determined by $p-\delta^2$ method proposed by M. Yoshiki (Reference 5). Figure 6 shows correlation between analytical results based on the present method and Y. Fujita's experimental results in which results obtained by Schlack were already plotted. It can be seen from this figure that end restraint condition of the side boundaries will give considerable influence on the buckling stress of perforated plates.

Furthermore it is interesting to note that the critical stress varies considerably depending on the ratio of the side length to diameter, that is, $r = c/a$. More precisely, $\bar{\sigma}_{cr}/\sigma_e$ decreases first from 4.00 at $r = 0$ to 3.67 at $r = 0.36$ and then increases monotonously up to 6.134 at $r = 0.7$ in case of Fujita's problem. Such an interesting behavior could be roughly

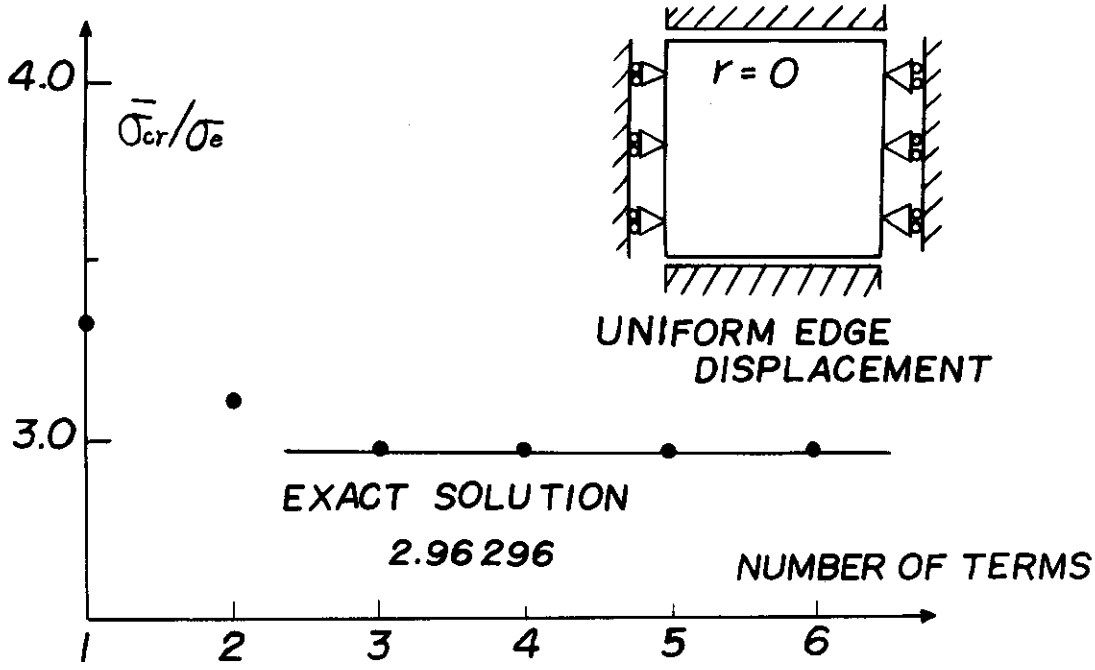

Figure 7. Convergency of Critical Stress to the Exact Solution (r = 0)

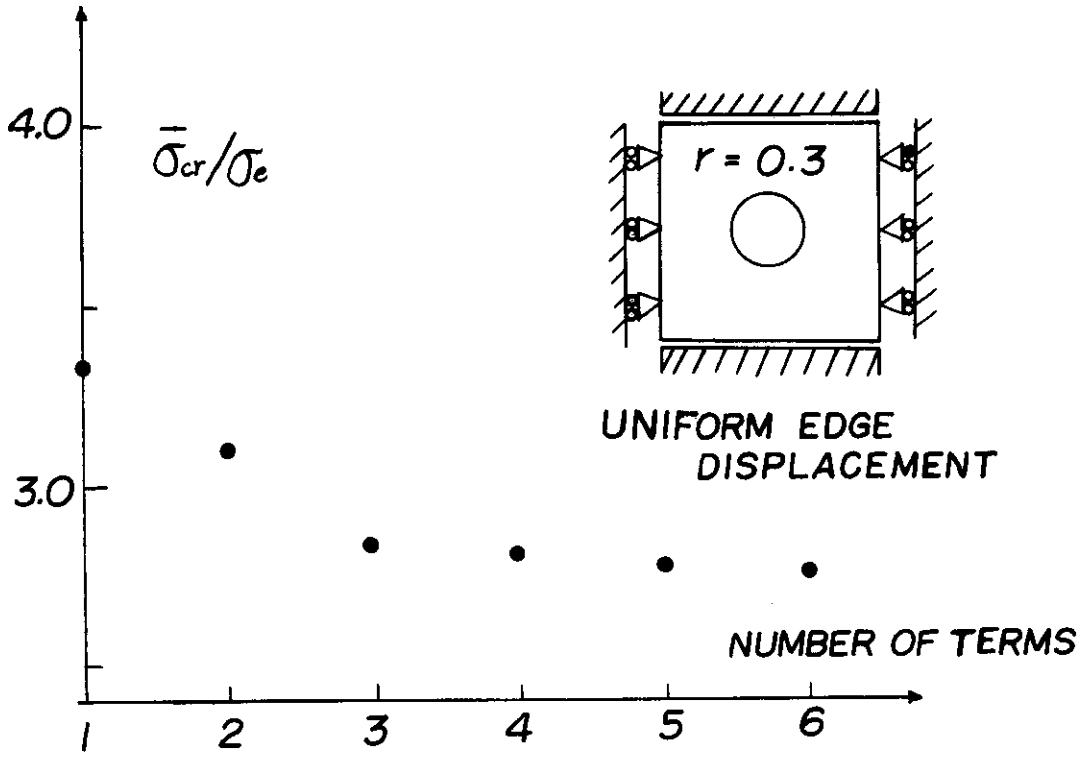

Figure 8. Convergency of Critical Stress (r = 0.3)

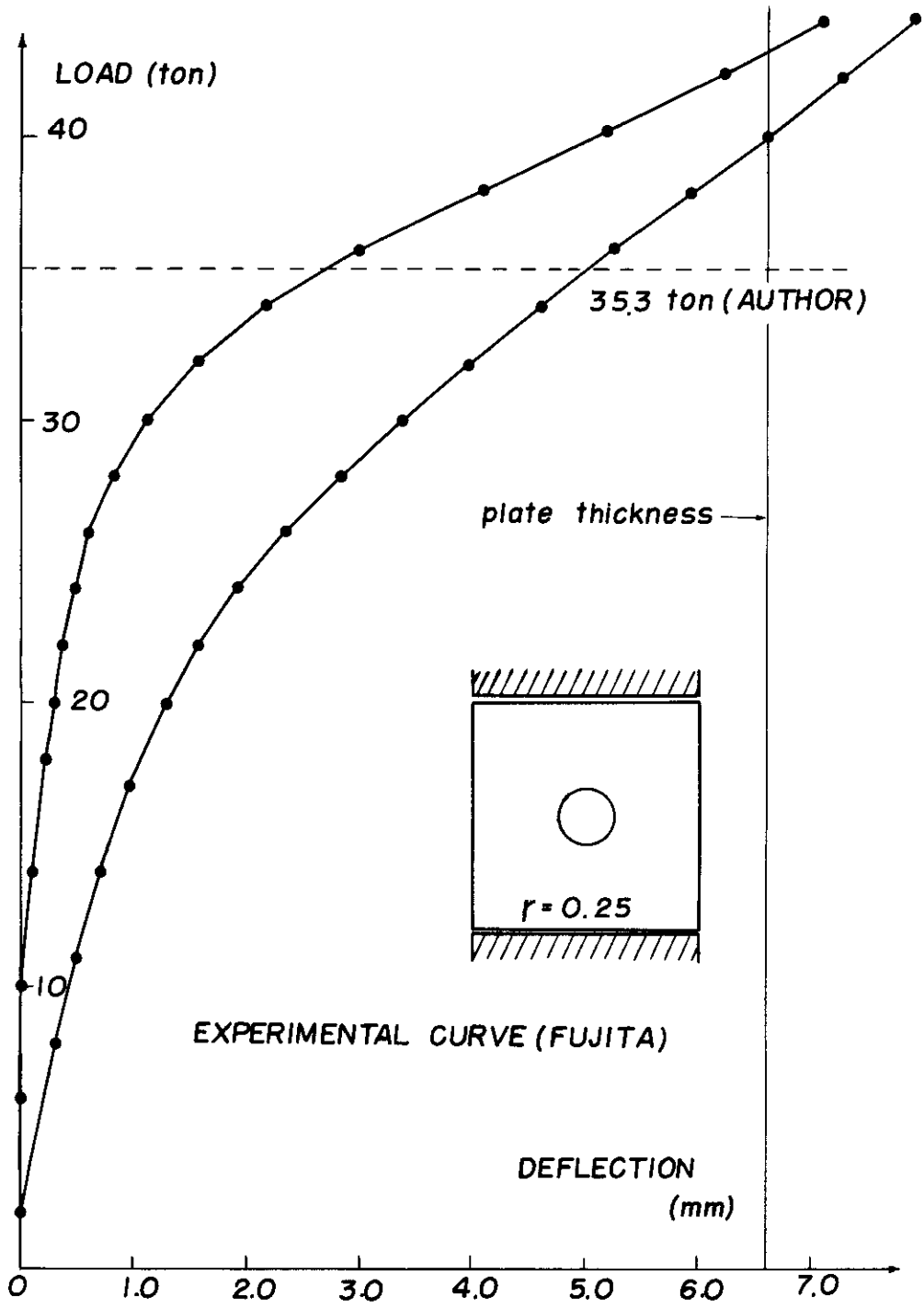

Figure 9. Experimental Load-Deflection Curve and Corresponding Calculated Critical Load of a Perforated Square Plate Subject to Uniform Edge Displacement (r = 0.25)

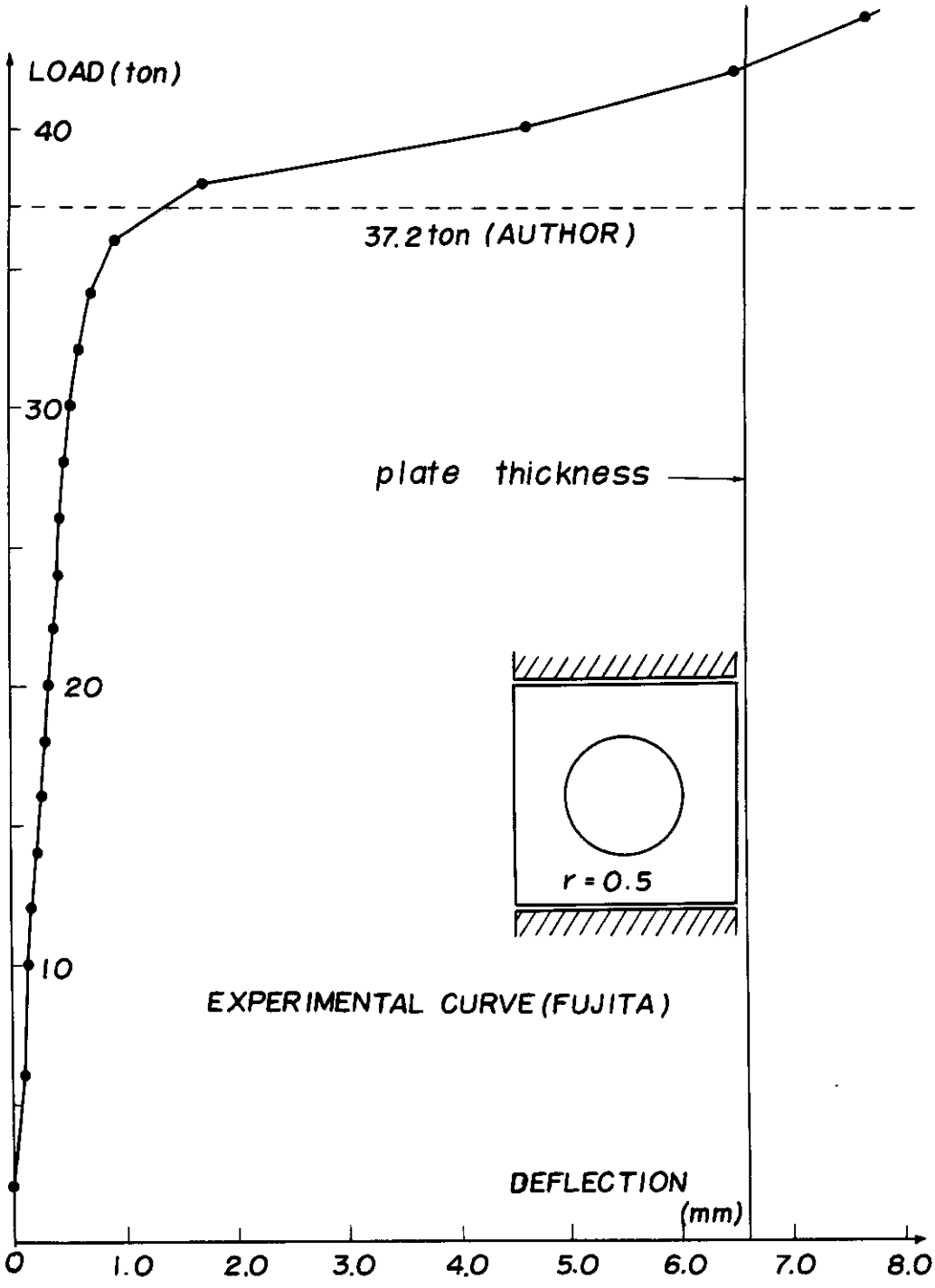

Figure 10. Experimental Load-Deflection Curve and Corresponding Calculated Critical Load of a Perforated Square Plate Subject to Uniform Edge Displacement (r = 0.5)

explained as follows: From examination of the stress distribution along the loading edges as shown in Figure 11, it can be seen that when r is comparatively larger, most of the applied load will be carried by the two narrow portions of a given plate whose width is $b = \frac{c-a}{2}$ along the side boundaries because of uniform edge displacement. Therefore the critical stress of the plate can be roughly approximated by the buckling stress of the simplified model as shown in Figure 12 and the results of analysis of this problem by S. Timoshenko, F. Hartman and E. Chwalla shows considerable increase of critical load when b becomes small.

Fairly good agreement between the calculated results and the experimental results can be observed also in this problem. It is also confirmed that the buckling modes with two axisymmetry always predominant among four possible buckling mode irrespective of r.

A Perforated Plate Subject to Uniform Edge Load

(Comparison with T. Kumai's study Reference 4)

For the last numerical analysis, a perforated plate under uniform edge load is also studied. In T. Kumai's study done in 1952, the boundary conditions of test plates are the same as that of Fujita's study except for the uniform loading condition along the edges: the lateral movement of the vertical edges are unrestrained, all edges are simply-supported and the plate is subject to uniform edge load along two parallel edges. The test plate is made of plexiglas (Young's modulus 290 to 300 kg/mm^2) and its dimension 100 x 100 x 1 mm. Tornament lever system was employed so as to obtain uniform distribution of the applied edge load. Approximate solution for the basic equation of a buckled plate was also obtained by the point-matching method in which the stress distribution inside of the plate was approximated by the stress distribution of an infinite plate with a circular hole at center under uniform uniaxial compression at infinity.

In this problem a fairly good agreement between the present theory and test results was also obtained as shown in Figure 13. From comparison of $\bar{\sigma}_{cr}/\sigma_e$ versus r = c/a curves, a distinct difference of the plate buckling strength under two different loading conditions i. e. uniform displacement and edge stress will be observed for the range of $0 \leqq r \leqq 0.7$. More precisely, the latter only shows the montonous decrease of $\bar{\sigma}_{cr}/\sigma_e$ with increase of r. For the range of the smaller hole, however, fairly good agreement of these two critical stress curves will be obtained, and this fact may be interpreted that the disturbance of a hole on the stress distribution will be quite local and almost the same stress distribution will be obtained for both cases.

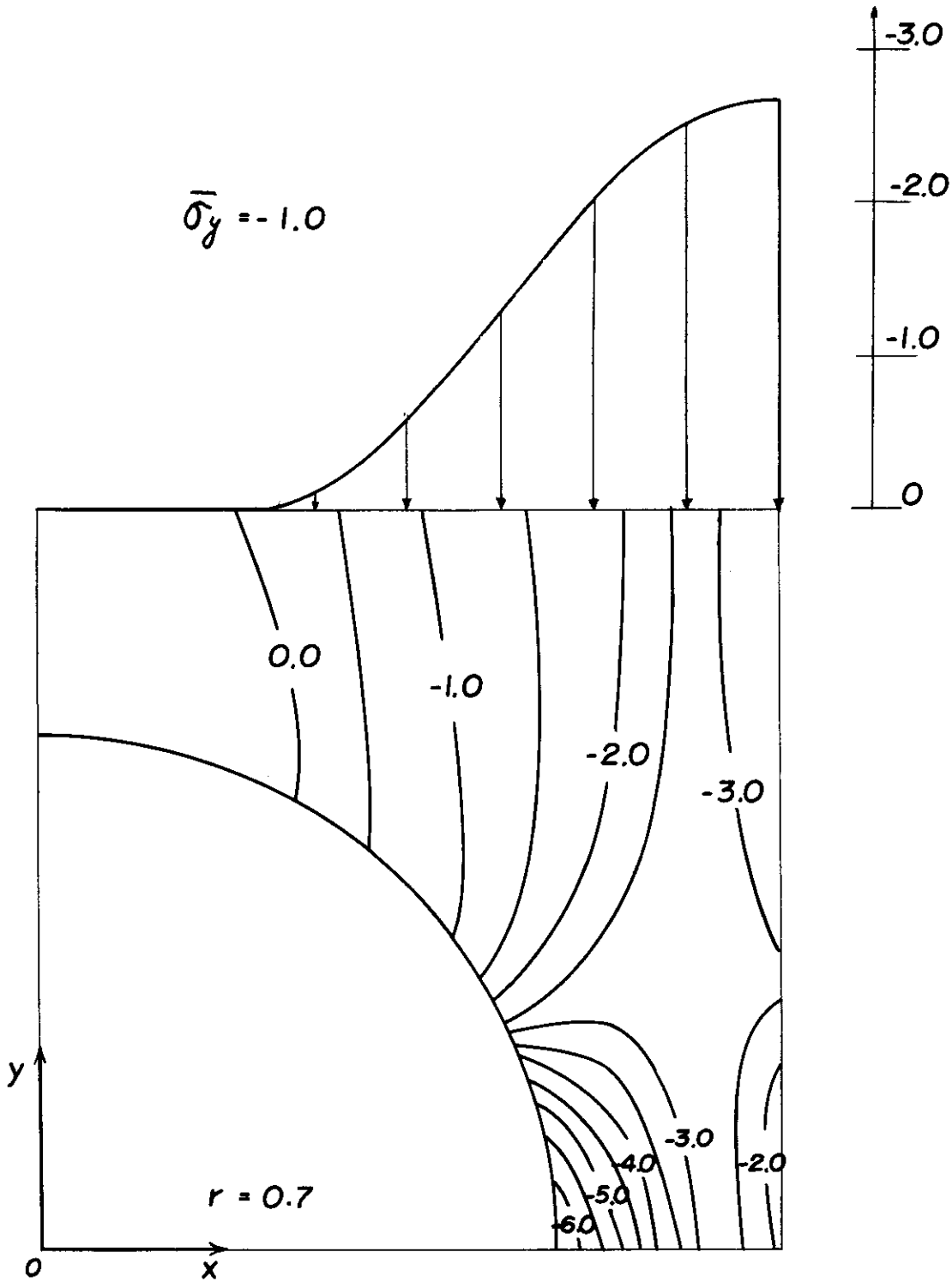

Figure 11. σ_y Distribution of a Perforated Square Plate Subject to Uniform Edge Displacement (II)

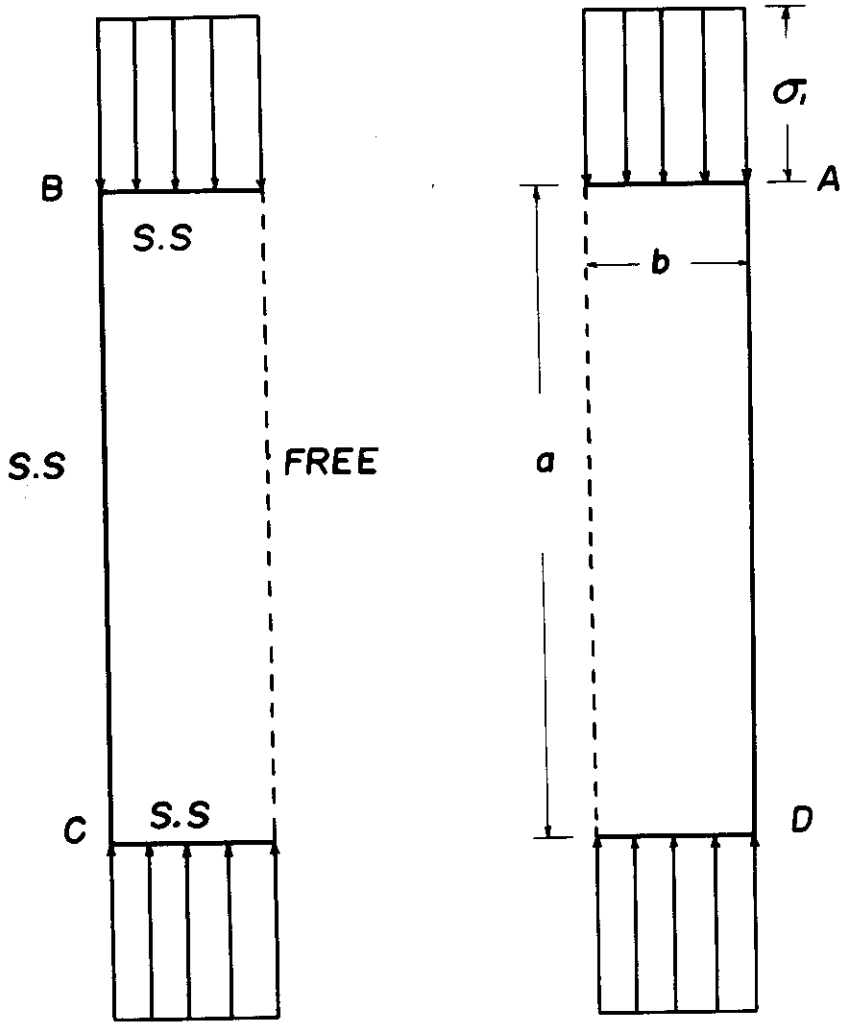

Figure 12. Simplified Model of Buckling Problem of a Square Plate with a Larger Hole

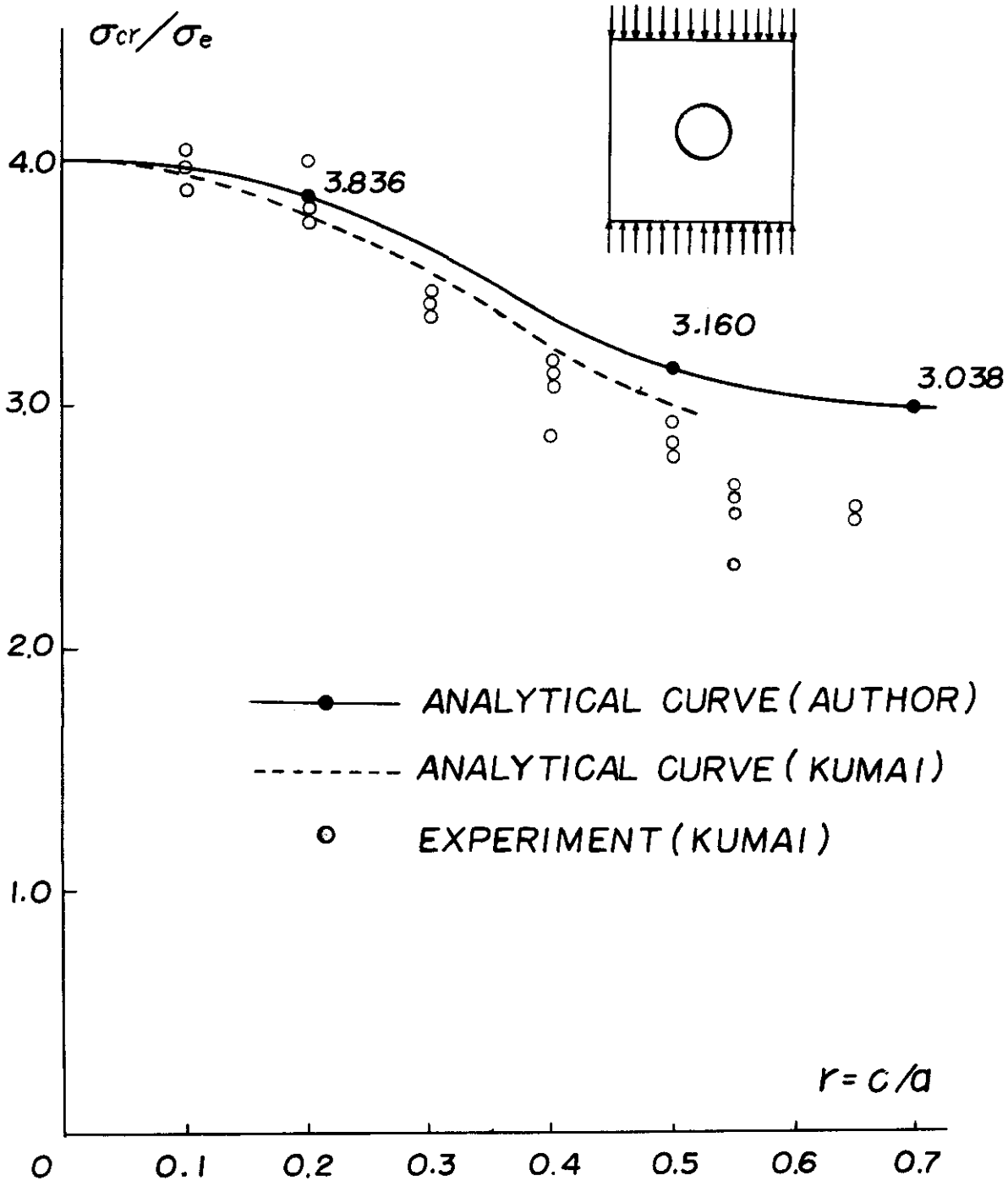

Figure 13. Critical Stress of a Simply-Supported Perforated Plate Subject to Uniform Stress Versus Diameter of Circular Hole

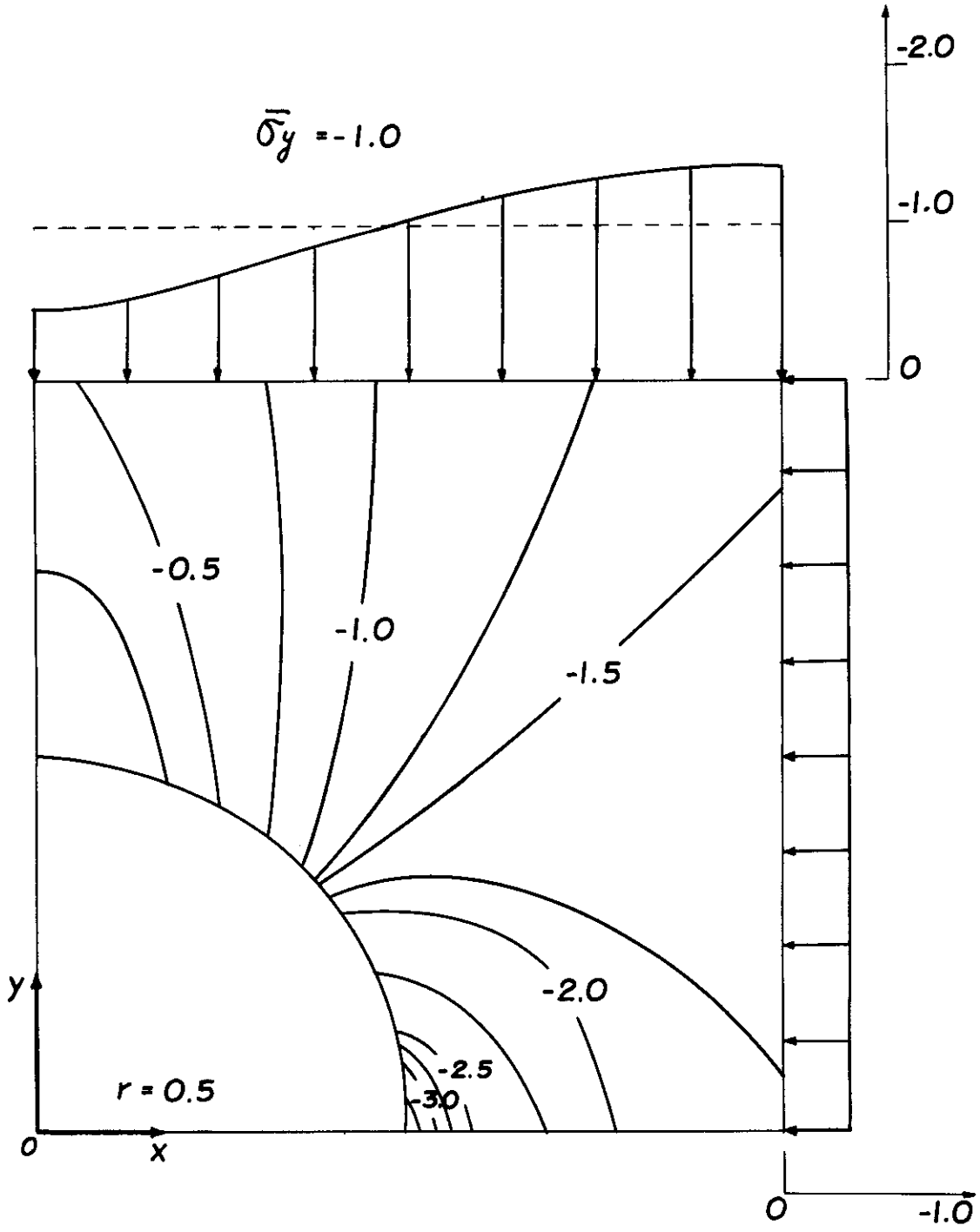

Figure 14. σ_y Distribution of a Perforated Square Plate Subject to Uniform Edge Displacement (I)

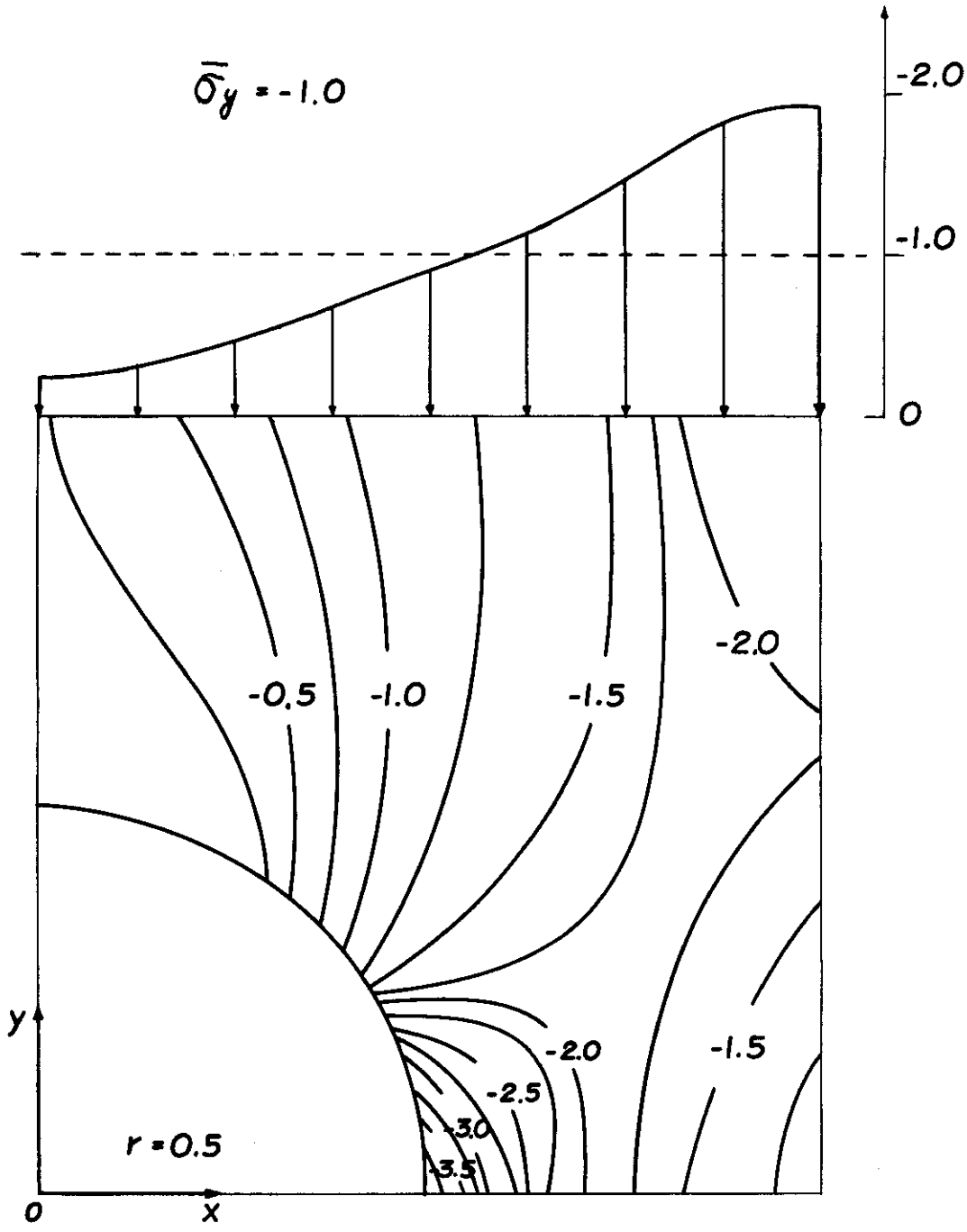

Figure 15. σ_y Distribution of a Perforated Square Plate Subject to Uniform Edge Displacement (II)

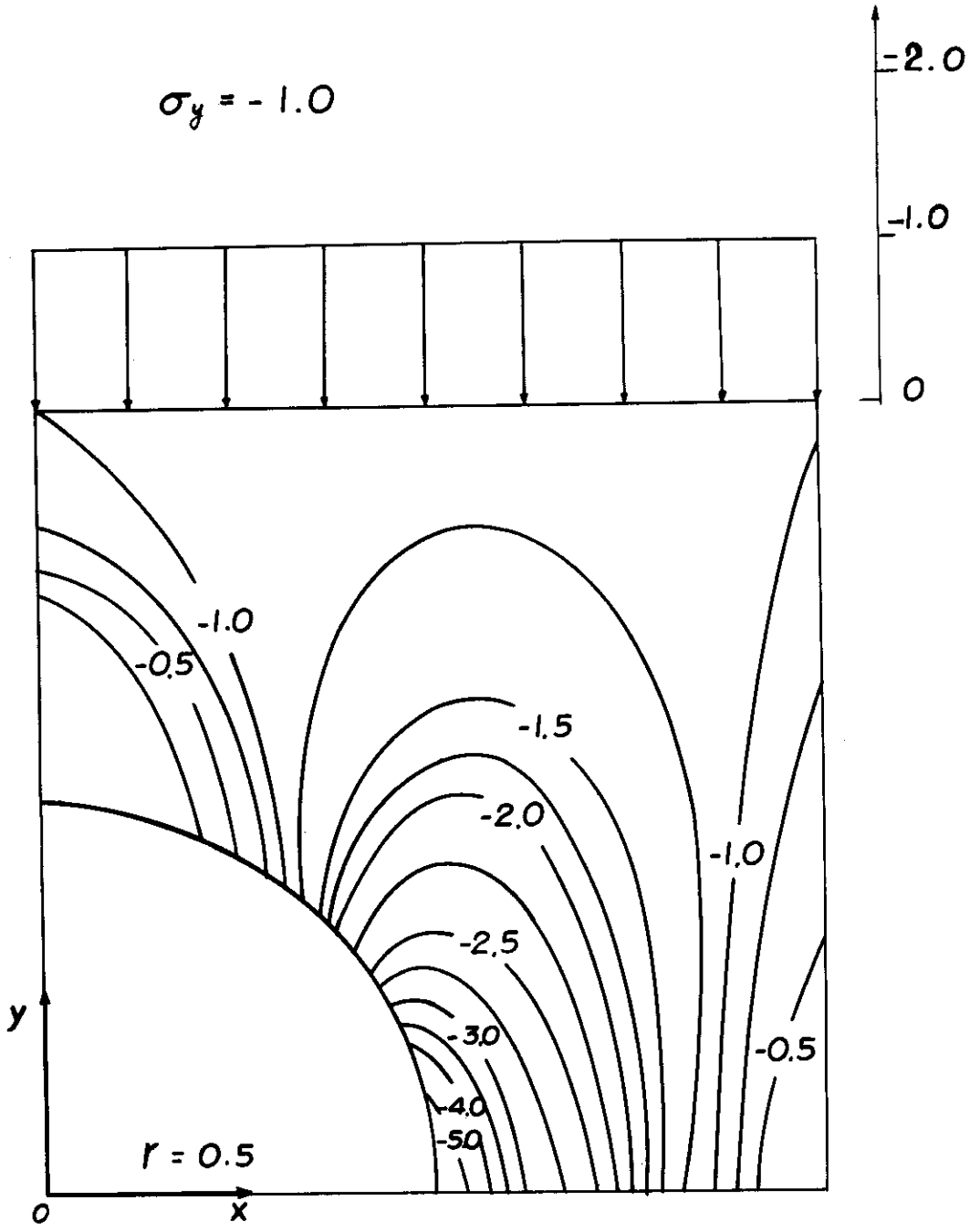

Figure 16. σ_y Distribution of a Perforated Square Plate Subject to Uniform Edge Stress

SECTION V

CONCLUSION

By combining the stress distribution obtained by the finite element method with the well-known Rayleigh-Ritz's procedure for plate buckling problems, a practical and standard method of solution for complicated plate buckling problems is proposed in this paper. From studies of various numerical examples on the buckling strength of perforated plates, it has been proved that the present method will be very powerful not only for buckling problems but also for any other plate problems with arbitrary plate shape and boundary conditions under arbitrary loading condition which are intractable by existing methods. Furthermore it is believed that such a combined use of energy procedure and the finite element method will find a vast range of application in the linear and nonlinear analysis of shell as well as plate structures.

SECTION VI

REFERENCES

1. M. Yoshiki and T. Kawai "On the Method of Application of Energy Principles to Problems of Elastic Plates" Proc. of 11th Internal Congress of Applied Mechanics, Springer Verlag, Berlin, 1967.

2. A. L. Schlack, Jr. "Elastic Stability of Pierced Square Plates" Experimental Mechanics, June 1964.

3. M. Yoshiki, Y. Fujita and Others "On the Buckling Strength of Perforated Plates (I)" Proc. of the Society of Naval Architects of Japan No. 122, Dec. 1967.

4. T. Kumai "Elastic Stability of the Square Plate with a Central Circular Hole Under Edge Thrust" Reports of Research Institute for Applied Mechanics Vol. 1, No. 2, April, 1952.

5. M. Yoshiki "A New Method of Determining the Critical Buckling Points of Rectangular Plates in Compression" Proc. of 1st Japan National Congress for Applied Mechanics 1951.